Dynamics of Antifreeze Glycoproteins in the Presence of Ice

Nelly M. Tsvetkova,* Brian L. Phillips,† Viswanathan V. Krishnan,** Robert E. Feeney,‡ William H. Fink,§ John H. Crowe,* Subhash H. Risbud,† Fern Tablin,¶ and Yin Yeh‖

*Section of Molecular and Cellular Biology and Departments of †Chemical Engineering and Materials Sciences, ‡Food Science and Technology, §Chemistry, ¶Anatomy, Physiology, and Cell Biology, and ‖Applied Science, University of California, Davis, California 95616 USA; and **Biology and Biotechnology Research Program, Lawrence Livermore National Laboratory, Livermore, California 94551 USA

ABSTRACT Antifreeze glycoproteins from the Greenland cod *Boreogadus saida* were dimethylated at the N-terminus (m*AFGP) and their dynamics and conformational properties were studied in the presence of ice using ^{13}C-NMR and FTIR spectroscopy. ^{13}C-NMR experiments of m*AFGP in D_2O, in H_2O, and of freeze-dried m*AFGP were performed as a function of temperature. Dynamic parameters (^{1}H $T_{1\rho}$ and T_{CH}) obtained by varying the contact time revealed notable differences in the motional properties of AFGP between the different states. AFGP/ice dynamics was dominated by fast-scale motions (nanosecond to picosecond time scale), suggesting that the relaxation is markedly affected by the protein hydration. The data suggest that AFGP adopts a similar type of three-dimensional fold both in the presence of ice and in the freeze-dried state. FTIR studies of the amide I band did not show a single prevailing secondary structure in the frozen state. The high number of conformers suggests a high flexibility, and possibly reflects the necessity to expose more ice-binding groups. The data suggest that the effect of hydration on the local mobility of AFGP and the lack of significant change in the backbone conformation in the frozen state may play a role in inhibiting the ice crystal growth.

INTRODUCTION

Antifreeze glycoproteins (AFGP) were first identified in Antarctic teleost fishes as the causative agents of freezing point depression of blood serum. AFGP were found to lower the freezing point by >1°C by a noncolligative mechanism, thus matching or exceeding the freezing point of sea water (for reviews see Feeney, 1988; Yeh and Feeney, 1996; Ewart et al., 1999).

The eight known fractions of AFGP, which range in molecular mass from 33.7 to 2.6 kDa (DeVries et al., 1970), have been characterized according to their size, with AFGP1 as the longest and AFGP8 as the shortest, respectively. Each fraction consists of a number of repeating units of alanine-alanine-threonine, with minor sequence variations. The threonines are glycosylated at the Cβ position with the disaccharide β-D-galactopyranosyl-(1,3)-2-acetamido-2-deoxy-α-D-galactopyranose. The longer glycopeptides, typified by AFGP2–5, are 20 times more active on a molar basis in lowering the freezing temperature of solution than the shorter ones, here represented as AFGP8 (see review in Feeney et al., 1986). Structurally, AFGP8 have proline in different positions following threonine, whereas AFGP2–5 exhibits a regular alanine-alanine-threonine sequence. Glycoproteins from the Greenland cod *Boreogadus saida* are studied in the present work. In AFGP8, alanine at positions 4 and 10 is substituted for proline, whereas in AFGP2–5 there are no proline residues.

In addition to AFGP, antifreeze proteins (AFP) are found in fish from the polar regions (for reviews see Davies and Hew, 1990; Sönnichsen et al., 1998; Harding et al., 1999; Haymet et al., 1999), insects (Duman et al., 1998; Liou et al., 2000; Graether et al., 2000), terrestrial arthropods (Duman, 2001), and plants (Doucet et al., 2000; Sidebottom et al., 2000). Although the structures of these AFP vary considerably, they have a common mechanism of noncolligative freezing-point depression and consequent inhibition of ice crystal growth (Raymond and DeVries, 1977; Raymond et al., 1989). Knight et al. (1991, 1993) showed that different types of AFP type I and AFGP bind to distinct ice crystal surfaces. A common feature that unites both AFGP and AFP is the lack of appreciable binding to the basal planes and adsorption primarily to the nonbasal planes of ice (Wen and Laursen, 1992; Wilson et al., 1993).

Because direct determination of the conformation and dynamics of AFGP at the ice-water interface remains a challenging experimental problem, one approach to test the postulated antifreeze mechanism with respect to AFGP is to examine their motional properties and secondary structure in the frozen state. ^{1}H- and ^{13}C-NMR (Bush et al., 1984; Bush and Feeney, 1986; Homans et al., 1985; Rao and Bush, 1987; Filira et al., 1990; Lane et al., 1998, 2000; Berman et al., 1980), Raman (Tomimatsu et al., 1976; Drewes and Rowlen, 1993), and infrared (Drewes and Rowlen, 1993; Lane et al., 2000) spectroscopic techniques have been applied to study the interactions of AFGP with liquid water. However, crystal growth experiments of ice in the presence of AFGP suggest that these proteins strongly affect the ice crystal morphology. Thus, understanding the interaction of AFGP with ice may provide closer insight into the mechanism of their antifreeze activity. This work presents a comprehensive study on the dynamics of AFGP in the presence of ice, based on experimental data obtained

Received for publication 31 July 2001 and in final form 28 September 2001.

Address reprint requests to Dr. Nelly Tsvetkova, Section of Molecular and Cellular Biology, University of California at Davis, Davis, CA 95616. Tel.: 530-752-1094; Fax: 530-752-5305; E-mail:nmtsvetkova@ucdavis.edu.

0006-3495/02/01/464/10 $2.00

using solid-state NMR and IR methods. To our knowledge, this is the first study on dynamic properties of AFGP in the presence of ice. ^{13}C-NMR spectra of AFGP show fast dynamics and high mobility in the frozen state. Using FTIR spectroscopy, we examined the local backbone conformation of both AFGP8 and AFGP2–5. The amide I region of the spectrum between 1700 and 1620 cm^{-1} arises from the stretching vibrations of the carbonyl group, which is sensitive to the local conformation (Byler and Susi, 1986; Dong et al., 1990; Prestrelski et al., 1991). The results show a high number of conformers in the presence of ice, suggesting high flexibility of the glycoprotein molecules.

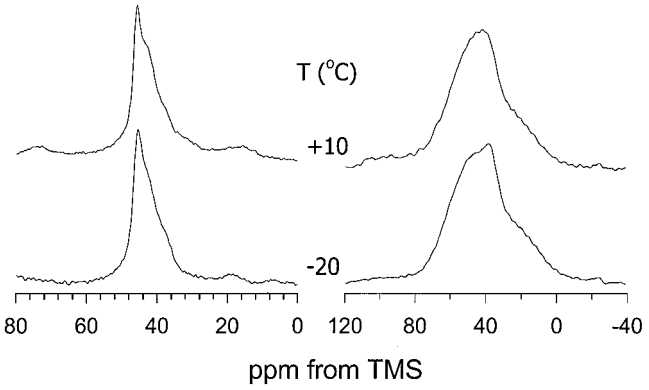

FIGURE 1 CP-MAS (*left*) and spin-echo (*right*) ^{13}C-NMR spectra of ^{13}C-methylated freeze-dried AFGP8.

MATERIALS AND METHODS

Antifreeze glycopeptides

AFGP from the Greenland cod *Boreogadus saida* were prepared as previously described (Feeney and Yeh, 1978; Osuga and Feeney, 1978). Fractions were assayed for antifreeze activity by measuring thermal hysteresis using a capillary freezing-melting point technique (DeVries, 1986).

Amino-terminus dimethylation

AFGP was dimethylated at the N-terminus according the method of Means and Feeney (1995). Briefly, AFGP in 0.2 M phosphate buffer (pH 7.5) were methylated with 1 M ^{13}C formaldehyde (Cambridge Isotope laboratories, Andover, MA) in the presence of 1 M borane dimethylamine (Sigma, St Louis, MO) as a reducing agent at 4°C. After the methylation the glycoproteins were dialyzed for 48 h to remove the excess of ^{13}C formaldehyde and borane dimethylamine, and lyophilized. The modified proteins are referred to as m*AFGP. The efficiency of the methylation was assessed by fluorescamine assay (Udenfriend et al., 1972). The lyophilized m*AFGP were mixed with H_2O or D_2O (Aldrich Chemical Company, Inc., Milwaukee, WI) (120 mg/ml). Before loading into the NMR rotor, the sample was frozen in small portions of 10 μl at relative humidity 0%.

Solid-state ^{13}C-NMR

The ^{13}C-NMR spectra were taken with a Chemagnetics CMX-400 spectrometer operating at 100.6 MHz and fitted with a standard double-resonance MAS probe configured for 7.5-mm-diameter rotors. The samples were held in MAS-NMR rotors with double o-ring sealed macor plugs. Single-pulse MAS and ^{13}C{^{1}H} CP-MAS spectra were taken at a spinning rate of 1.6 kHz with standard pulse sequences. The RF field strength was 32 kHz for both ^{1}H decoupling and cross-polarization. Typical acquisition parameters include pulse widths of 6–8 μs, relaxation delays of 0.5 s, and a contact time of 1 ms (CP-MAS). Static (nonspinning) spectra were taken with a spin echo sequence (90-τ-180-τ-acquire) with a 50-μs interpulse delay (τ). The relaxation times for ^{13}C{^{1}H} cross-relaxation (T_{CH}) and ^{1}H spin-lattice relaxation in the rotating-frame (^{1}H $T_{1\rho}$) were measured from intensity changes upon varying the CP-MAS contact time from 0.1 to 20 ms, assuming single-exponentials for both cross-polarization and relaxation processes. Nonlinear least-square fits to the experimental data points by standard protocols are used to obtain T_{CH} and $T_{1\rho}$ values. High-power proton decoupling was used only during acquisition. Temperatures were controlled by flowing chilled, dry air or N_2, heated to the desired temperature, over the sample. Temperatures were calibrated against the $PbNO_3$ chemical shift thermometer (van Gorkom et al., 1995), and the total temperature gradient across the sample was ~3°C. Chemical shifts are reported relative to TMS via the methyl resonance of hexamethylbenzene, taken to be +17.36 ppm. NMR experiments of m*AFGP were performed at three different sample conditions: freeze-dried, in 100% D_2O, and in 100% H_2O.

FTIR spectroscopy

Infrared spectra of AFGP were recorded using a Perkin-Elmer 2000 FTIR spectrometer (Perkin-Elmer, Norwalk, CT) equipped with a liquid nitrogen-cooled mercury/cadmium/telluride (MCT) detector. About 2 μl of protein solution was loaded on CaF_2 windows (Wilmad Glass Co., Buena, NJ). The temperature of the sample was controlled using a Peltier device (Paige Instruments, Davis, CA) and monitored separately by a thermocouple located on the sample windows. Spectra were recorded at temperature increments of 1.5°C/min. The optical bench was purged with CO_2 free air. For each spectrum 18 interferograms were collected at 4 cm^{-1} resolution and 3600–900 cm^{-1} wavenumber range. For aqueous and frozen samples, reference spectra of liquid and frozen water were recorded and subtracted from the observed protein spectra according to Dong et al. (1990). Spectral analysis was carried out using the analytical software Spectrum 2000 (Perkin-Elmer). Curve-fitting of the original absorbance spectra was performed assuming Gaussian band shapes for the deconvolved components.

RESULTS

^{13}C-NMR

The ^{13}C-NMR spectra of freeze-dried m*AFGP8 under static and magic angle spinning (MAS) conditions at +10° and −20°C are shown in Fig. 1. Fig. 2 shows the ^{13}C-MAS-NMR spectra (*left*) and the corresponding static (nonspinning) spectra (*right*) of m*AFGP in the presence of D_2O as a function of temperature. Spectra of the protein obtained under the same conditions but in the presence of H_2O are shown in Fig. 3. The NMR spectrum shown in the top row of the left panel of Fig. 2 was acquired on the same sample, but at +20°C, and corresponds to the solution state.

Solid-state MAS-NMR spectra of freeze-dried m*AFGP8 (residual water content of 4 w. %) at +10 and −20°C are very similar (Fig. 1). Further lowering of temperature to −80°C does not produce any significant difference in their overall appearance (data not shown).

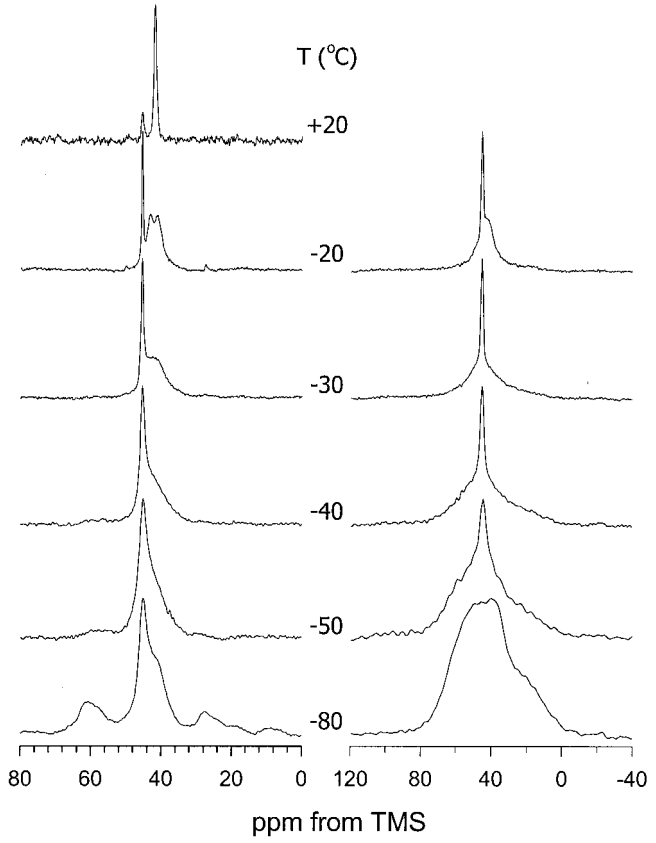

FIGURE 2 CP-MAS (*left*) and spin-echo ^{13}C-NMR (*right*) spectra of ^{13}C-methylated AFGP8 in D_2O as a function of temperature.

The ^{13}C-MAS-NMR spectrum of m*AFGP8 at +20°C in D_2O (Fig. 2, *left*), exhibits two principal resonances, at 45.5 and 42.1 ppm in an approximate intensity ratio of 1:4. Upon lowering the sample temperatures to freezing conditions, additional splitting of peak at 42 ppm is observed, suggesting that conformational states of these sites are freezing out. This splitting corresponds to distinct chemical environments seen by the two C-terminal methyl groups of m*AFGP8, with one methyl carbon shielded more by the carbonyl carbon. The hindered rotation about the N–C bond in the C-terminal seems to introduce this unexpected feature in the NMR spectrum. Further decreasing of the temperature leads to considerable broadening of these peaks (broad peak) predominantly due to freezing of additional conformational states below −30°C. Hence, these two peaks are referred to hereafter as sharp (downfield, at 45.5 ppm) and broad (upfield, at 42 ppm), respectively. In contrast, the sharp peak (45.5 ppm) does not show any additional splitting upon lowering temperatures, except for normally expected characteristic broadening of the resonance. These results suggest that the ^{13}C-labeled dimethyl groups at the N-terminal of AFGP undergo significant chemical exchange between various equivalent conformations and that some of these conformations freeze out at lower temperatures. In the present study we are using these two features as indicative of a temperature-sensitive environment of the methylated N-terminus without undertaking a detailed treatment of the exchange kinetics. A more complete analysis of this kinetics will be presented elsewhere. The exchange dynamics of the broad peak is more influenced by the freezing than that of the sharp peak.

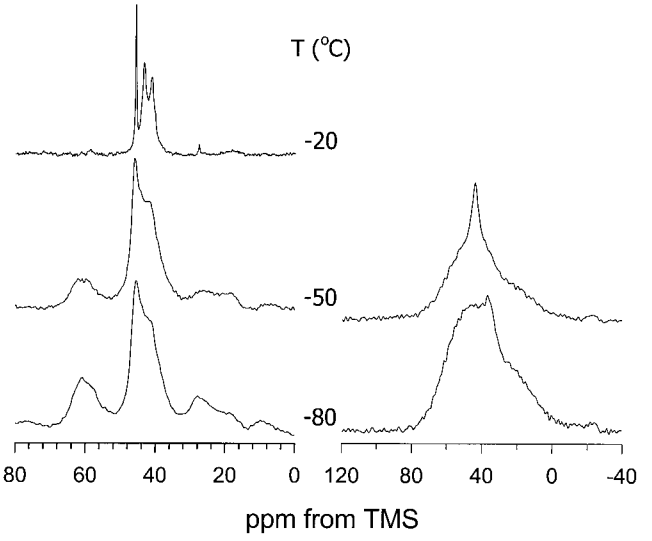

FIGURE 3 CP-MAS (*left*) and spin-echo ^{13}C-NMR spectra (*right*) of ^{13}C-methylated AFGP8 in H_2O as a function of temperature.

Table 1 summarizes the ^{1}H $T_{1\rho}$ and T_{CH} values estimated using contact time-dependent CP-MAS experiments on the freeze-dried, D_2O-, and H_2O-saturated m*AFGP8. The chemical shifts of the sharp peaks are at ~45 ppm, while those of the broad peak and its additional components that appear upon freezing are at ~41.5 ppm. Within the experimental error, the chemical shifts of the peaks in all three different samples are close to each other. The samples were cooled slowly with sufficient delay for temperature stability to minimize any systematic errors due to temperature gradients. ^{1}H $T_{1\rho}$ and T_{CH} for the broad peak are estimated in all the samples and at all temperatures (Table 1), whereas these parameters could not be estimated for the sharp peak

TABLE 1 Relaxation times for ^{13}C{^{1}H} cross-polarization dynamics

	Temperature	δ (ppm)	$T_{1\rho}$ (ms)	T_{CH} (ms)
m*AFGP8/D_2O	−20°C	41.1, 42.9	2.6	0.27
		45	>20	>20
	−80°C	42.0	13.5	0.15
		45	14.5	0.20
m*AFGP8/dried	−20°C	42	3.7	0.11
		45	3.7	0.12
m*AFGP8/H_2O	−20°C	41.2, 43.3	3.8	0.33
		45	>20	>20
	−80°C	42	1.4	0.10
		45	1.6	0.14

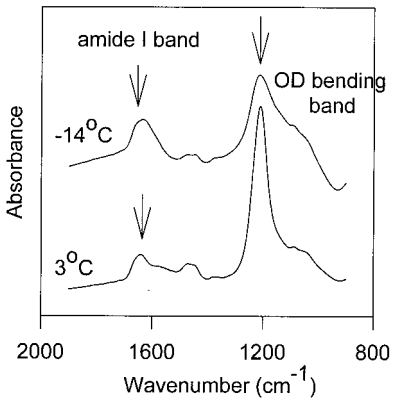

FIGURE 4 IR spectra of AFGP8 in D_2O (56 mg/ml) at 3°C and −14°C.

at −20°C for m*AFGP in H_2O or D_2O. Significant differences in both $T_{1\rho}$ and T_{CH} values are observed between the different samples, suggesting a dominant influence of protein hydration and interaction between ice and m*AFGP molecules.

Traces of the natural abundance backbone carbon resonances, most likely from the methyl groups of alanine in AFGP8, are observed at the ^{13}C-NMR spectrum at −20°C (27 ppm, Fig. 2, *right*). These resonances are not detected in the ^{13}C-CP-MAS spectra, suggesting an efficient self-decoupling between ^{1}H and ^{13}C spins at this temperature.

In the frozen state, the sharp peak broadens gradually in the MAS-NMR spectra with decreasing temperature, from 0.4 ppm (full-width at half-maximum, FWHM) at −20°C to ~2 ppm at −80°C, and remains distinctly narrow to below −50°C in the spin-echo spectra (Fig. 2, *left*). This result suggests considerable mobility for this conformer, even at temperatures where the fluid boundary layer is probably frozen. The relaxation times determined from the ^{13}C{^{1}H} cross-polarization dynamics (Table 1) also suggest considerable mobility for the methyl groups. At −20°C, the ^{13}C-^{1}H cross-relaxation time (T_{CH}) and ^{1}H $T_{1\rho}$ are very long (>20 ms) in both H_2O and D_2O, indicating self-decoupling of both the labeled methyl carbons from the protons and the methyl protons from other hydrogens on the protein and in the ice. At −80°C the T_{CH} values are much shorter, 0.15 ms, and similar to that obtained for the freeze-dried sample at −20°C. The principal effect of the presence of protons of water is a decrease of the ^{1}H $T_{1\rho}$ from ~14 ms in D_2O ice to 1.6 ms in the presence of H_2O ice, indicating possible spin exchange between the protons of the protein and the water.

The broad peak (near +42 ppm) displays a markedly different behavior as a function of temperature. The width of the ^{13}C MAS-NMR peaks increases significantly with decreasing temperature, from ~2.5 ppm (FWHM) near −20°C to ~9 ppm at −50°C (Fig. 2, *left*). The two distinct resonances cannot be resolved below ~−25°C. From −50°C to −80°C the peak width remains approximately constant, but the spinning sideband intensity increases significantly, suggesting onset of strong dipolar coupling to protons, probably owing to recoupling to the methyl protons resulting from reduced flexibility. Spectra taken under nonspinning conditions (Figs. 2 and 3 *right*) show a nearly uniaxial chemical-shift-anisotropy (CSA) powder pattern at temperatures below −40°C, suggesting a significantly reduced motion of the methyl groups. The T_{CH} and $T_{1\rho}$ values of AFGP8 measured at −20°C in the presence of D_2O for this downfield resonance exhibit shorter values (T_{CH} = 0.27 ms and ^{1}H $T_{1\rho}$ = 2.6 ms) than for the peak at +45 ppm, owing to more restricted motions.

These relaxation times are somewhat longer in H_2O (T_{CH} = 0.33 ms; ^{1}H $T_{1\rho}$ = 3.8 ms), indicating that the principal difference between the presence of D_2O or H_2O is slightly more mobility in H_2O; the spins on the methyl groups appear to be decoupled from those in the solvent at this temperature. At −80°C, however, the relaxation times for the broad peak are the same as those for the sharp peak, within experimental uncertainty. That the T_{CH} values are similar in H_2O, D_2O, and in the freeze-dried state indicates

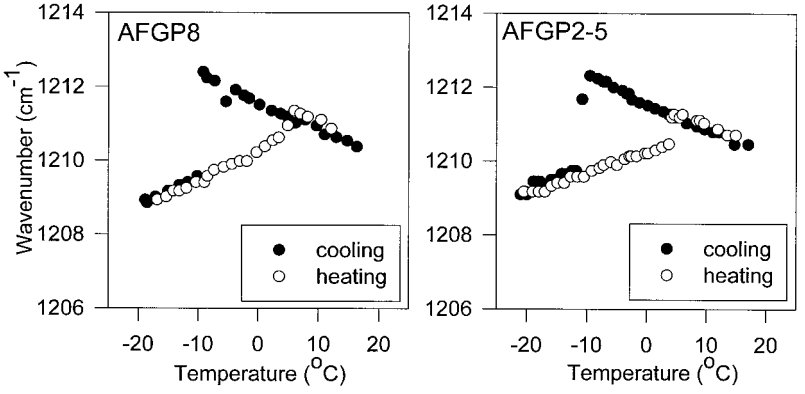

FIGURE 5 Freezing and melting profiles of AFGP8 in D_2O (56 mg/ml), and of AFGP2–5 in D_2O (56 mg/ml) monitored by changes in the wavenumber of the OD bending band at ~1200 cm^{-1}.

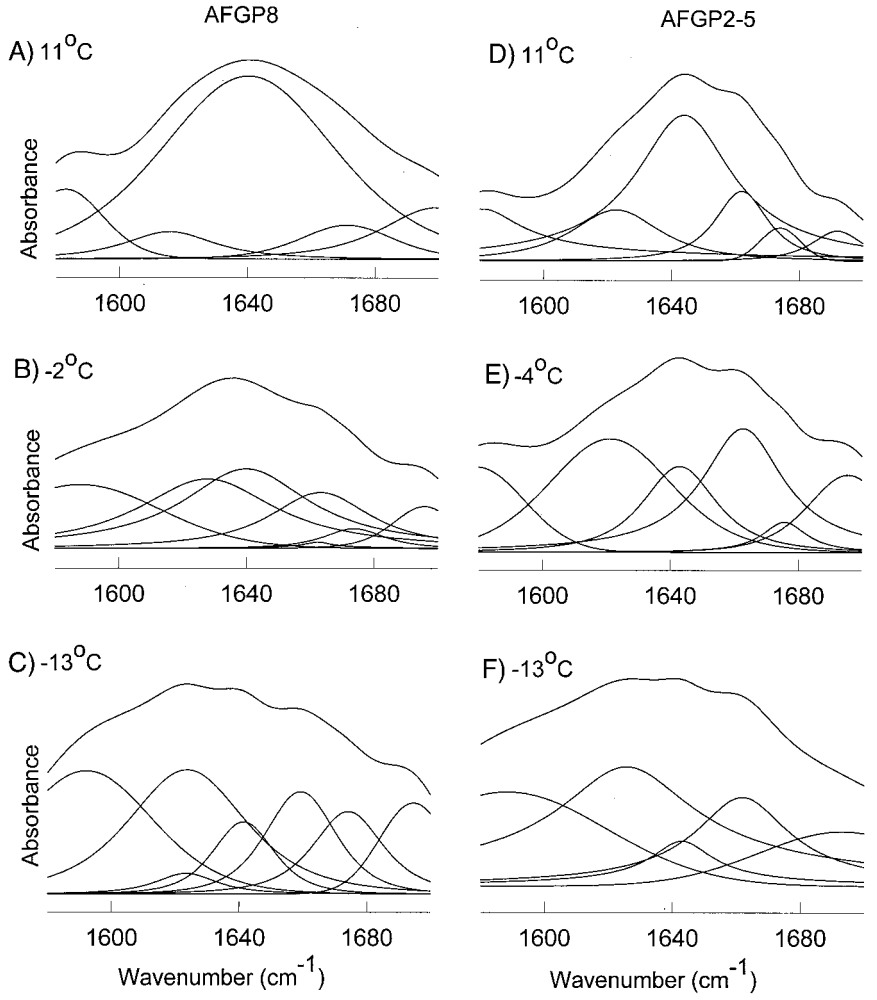

FIGURE 6 Deconvolved amide I bands of AFGP8 (*left*) and AFGP2–5 (*right*) in D_2O with fitted component bands. Spectra were recorded as described in Materials and Methods.

polarization transfer primarily from the methyl protons to the labeled carbons in the rigid limit at this temperature, corresponding to freezing-in of most large-scale molecular motions. The differences in ^1H $T_{1\rho}$ among these samples at −80°C can be related to spin-exchange between the methyl protons and H_2O solvent, and among the proteins in the freeze-dried sample. The temperature dependence of the NMR spectra of m*AFGP2–5 is very similar to that of m*AFGP8 (data not shown).

FTIR

FTIR provides information about conformation of the protein backbone via the frequency of the amide I band between 1700 and 1620 cm^{-1} that arises primarily from stretching vibrations of the backbone C═O groups. The frequency of these vibrations has been shown to be sensitive to the molecular geometry and hydrogen-bonding characteristics of the peptide backbone, and specific conformational types give rise to discrete bands in the amide region (Bandekar, 1992; Byler and Susi, 1986). Fig. 4 shows typical spectra of AFGP8 in D_2O at 3°C (in the liquid state) and at −14°C (in the frozen state). Since the amide I band appears featureless, deconvolution and curve-fitting were applied to resolve the individual amide I components (Byler and Susi, 1986; Surewicz and Mantsch, 1988). However, the precise assignment of bands to secondary structure type remains controversial (Surewicz et al., 1993).

Freezing and melting of AFGP8 and AFGP2–5 in D_2O are monitored by the spectral changes of the OD bending band of D_2O at 1200 cm^{-1} (see Fig. 4), and the results are displayed in Fig. 5. During freezing, the intensity of this band decreases and the peak position shifts to lower frequency. Spectra in the amide I band of AFGP8 and AFGP2–5 in solution, at supercooled temperature (supercooling refers to a liquid below the freezing point and is observed between 4 and −10°C in this system) and in the frozen state are shown in Fig. 6. Tables 2 and 3 list the peak

TABLE 2 Peak positions (cm^{-1}), relative areas (%), and apparent secondary structures of AFGP8 in D_2O, in a supercooled state, and in the presence of ice

	Wavenumber (cm^{-1})	Relative Area (%)	Secondary Structure type
Liquid	1618 ± 1	5 ± 2	Polyproline*
Supercooled	—	—	
Solid	—	—	
Liquid	—	—	
Supercooled	1629 ± 1	24 ± 8	Extended†‡
Solid	1627 ± 2	27 ± 3	Extended‡§
Liquid	1642	68 ± 6	Unordered*†‡¶‖
Supercooled	1642 ± 2	36 ± 8	Unordered*†‡¶‖
Solid	1642 ± 1	13 ± 4	Unordered*†‡§¶‖
Liquid	—	—	
Supercooled	1663 ± 2	14 ± 5	Turns†‡¶‖
Solid	1660 ± 1	24 ± 1	Turns§
Liquid	1672 ± 2	7 ± 2	Extended†‡¶
Supercooled	1674 ± 1	12 ± 3	Extended†‡¶‖
Solid	1674	18 ± 4	Extended†‡§¶‖
Liquid	1698 ± 2	20 ± 5	Turns†‡¶‖
Supercooled	1695 ± 2	14 ± 6	Turns†‡¶‖
Solid	1694 ± 2	18 ± 2	Turns†‡§¶‖

*Assigned in Lane et al. (2000).
†Assigned in Surewicz and Mantsch (1988).
‡Assigned in Byler and Susi (1986).
§Assignments proposed or corroborated from this study.
¶Assigned in Prestrelski et al. (1991).
‖Assigned in Dong et al. (1990).

TABLE 3 Peak positions (cm^{-1}), relative areas (%), and apparent secondary structures of AFGP2-5 in D_2O, in a supercooled state, and in the presence of ice

	Wavenumber (cm^{-1})	Peak Area (%)	Secondary Structure Type
Liquid	1619 ± 2	15 ± 2	Polyproline*
Supercooled	1620 ± 2	35 ± 7	Polyproline*
Solid	—	—	
Liquid	—	—	
Supercooled	—	—	
Solid	1625 ± 2	50 ± 4	Extended†
Liquid	1644 ± 1	37 ± 4	Unordered‡§¶‖
Supercooled	1644 ± 1	34 ± 5	Unordered‡§¶‖
Solid	1643 ± 1	16 ± 4	Unordered*†‡§¶‖
Liquid	1661 ± 2	29 ± 3	3_{10} Helix*‖
Supercooled	1661 ± 2	20 ± 4	3_{10} Helix*‖
Solid	1661 ± 1	17 ± 3	3_{10} Helix*†‖
Liquid	1674 ± 2	10 ± 1	Extended‡§¶
Supercooled	1675 ± 2	8 ± 4	Extended‡§¶
Solid	—	—	
Liquid	1693 ± 2	3 ± 1	Turns‡§¶
Supercooled	1695 ± 1	7 ± 4	Turns‡§¶
Solid	1694 ± 2	17 ± 4	Turns†‡§¶

*Assigned in Lane et al. (2000).
†Assignments proposed or corroborated from this study.
‡Assigned in Surewicz and Mantsch (1988).
§Assigned in Byler and Susi (1986).
¶Assigned in Prestrelski et al. (1991).
‖Assigned in Dong et al. (1990).

positions and areas relative to the total area of the amide I region calculated by curve-fitting the deconvoluted spectra. For both types of glycoproteins, the spectra in liquid and frozen state are quite different. In solution, the predominant feature of the deconvolved amide I band of AFGP8 is the intense peak at 1642 cm^{-1} assigned to unordered conformation (Fig. 6 *a*, Table 2) (Byler and Susi, 1986; Surewicz and Mantsch, 1988; Prestrelski et al., 1991). Two additional bands at 1618 and 1672 cm^{-1} are assigned to polyproline II (Lane et al., 2000) and extended β structures (Byler and Susi, 1986; Surewicz and Mantsch, 1988), respectively. Fig. 6 *a* also shows peaks arising from the side chain vibrations (Chirgadze et al., 1975) fitted at 1590 cm^{-1}. We are including these peaks in the curve-fitting analysis to avoid the approximation otherwise incurred with the addition of a sloping baseline parameter. These peaks are not part of the amide I region and therefore are not used in calculating the relative intensities of its components.

Examination of the amide I band of AFGP8 in the supercooled and frozen state (Fig. 6, *b* and *c*) shows numerous bands corresponding to extended conformation and turns (Table 2). In addition, the band at 1642 cm^{-1} assigned to unordered structure decreases in intensity in the frozen state.

The amide I region of the spectrum of AFGP2–5 in solution is dominated by a band at 1644 cm^{-1} corresponding to unordered conformation (Byler and Susi, 1986; Surewicz and Mantsch, 1988; Prestrelski et al., 1991), which decreases in intensity in supercooled and frozen AFGP2–5 (Fig. 6, *d–f*; Table 3). In addition, the band at 1661 cm^{-1} assigned to 3_{10} helix in solution (Dong et al., 1990; Lane et al., 2000) increases in intensity upon freezing. Along with 3_{10} helical structure, extended β conformation and turns appear to dominate the secondary structure of AFGP2–5 similarly to AFGP8, suggesting that the two types of antifreeze glycoproteins differ mainly in the distribution of possible conformers. This may be associated with the influence of the proline residues on the AFGP8 conformation, producing a local order in the polypeptide backbone (Lane et al., 1998).

In conclusion, the FTIR data of AFGP8 and the higher-molecular weight homologs lacking proline provide no evidence for a single dominant secondary structure. During freezing, the structural order reflected in the higher percentage of turns and extended β conformation increases. The range of possible conformers of these molecules in the presence of ice suggests a very high flexibility. One possible role of the high flexibility could be to circumvent the necessity for binding to a flat surface. Another possibility could be to expose more ice-binding groups.

DISCUSSION

The discovery of antifreeze glycoproteins 30 years ago has opened up an exciting field of research into the role of these proteins in inhibiting the growth of ice at subzero temperatures. Despite the significant amount of work and extensive reviews from many disciplines from ice physics to molecular biology and physiology, little is known about the structure and dynamics of these proteins in the presence of ice. The lack of information is mainly due to difficulties of the existing experimental methods in obtaining details at the molecular level. Furthermore, there are few methods that are sensitive enough to measure consistent and reliable parameters at low temperatures. An additional difficulty in determining the three-dimensional structures of AFGP is inherent to the presence of glycosylated sugar residues. Glycoproteins are generally not amenable for crystallization and are difficult to overexpress in cell lines, and conventional tools for structure determination by x-ray diffraction have thus far failed. The combination of FTIR and solid-state NMR provides a powerful tool for studying the overall secondary structure and local dynamics of AFGP molecules in the presence of ice.

Chemical modification and antifreeze activity

The N-terminal alanine of AFGP is modified to ^{13}C-labeled *N*,*N*-dimethylalanine (see Materials and Methods). This approach greatly increases the sensitivity of the ^{13}C signals and allows us to obtain specific motional information. The site-directed methylation of the AFGP N-terminus is very important for this investigation because any other method for chemical modification, for example altering the hydroxyl groups of the side chain sugar residues, may interfere with the antifreeze activity of the protein (Komatsu et al., 1970). Modification of the N-terminal of the protein by methylation has been shown to have no effect on the antifreeze activity (Geoghegan et al., 1980). In addition, this modification does not affect either the backbone or side chain conformation of the protein, thus allowing us to attribute the observed change in the dynamics of the methyl groups to that of AFGP and its interaction with ice.

Protein conformation in the solid state

Lane et al. (1998, 2000) have recently investigated the structure and dynamics of AFGP in the solution state. Their results suggest a structural model of a protein that corresponds to an extended backbone undergoing significant segmental motion. However, smaller segments of the protein containing the repeats Ala-Thr-Pro-Ala adopt a well-defined conformation with no long-range order. In these experiments, the lack of long-range order is determined on the basis of the absence of nuclear Overhauser effects (NOE), which are normally expected for peptides of this size at room temperature. In addition, the authors observed an extensive hydration of the protein.

The solid-state NMR results presented here are dominated by the local differences in the conformation of m*AFGP at the N-terminus. However, complementary FTIR experiments (Fig. 6) are used to address changes in the secondary structure. Although the FTIR data (Tables 2 and 3) do not provide evidence for marked conformational changes of the protein backbone upon freezing, there is a preference for certain conformations. The high number of structures observed for the two types of glycoproteins (Tables 2 and 3) in the liquid state is in general agreement with those reported earlier using FTIR (Lane et al., 2000). Random, unordered conformation appears to dominate the secondary structure in AFGP8, whereas both random and 3_{10} helix are the main conformations in AFGP2–5 in the liquid state. In the supercooled state, in AFGP8, the percentage of unordered structure markedly decreases, while that of the extended structure and turns increases. In AFGP2–5, however, in the supercooled state, the unordered conformation is still dominating the secondary structure, although the percentage of 3_{10} helix is reduced. In the presence of ice, a high percentage of turns and extended structure in both types of glycoproteins is observed, possibly reflecting a higher extent of molecular order. Thus, although a proline residue may affect the local conformational flexibility (Lane et al., 1998), it does not appear to be essential for the formation of different conformers in the presence of ice.

Dehydrated AFGP

The way a protein molecule adopts a specific three-dimensional structure may not be solely determined by its amino acid sequence, but also by the environment in which it resides. It is not known whether AFGP adopts a particular structure in the dehydrated state and whether it corresponds to its native structure (native structure is defined as the conformational state where it is functional). One way to address this issue is to follow changes in the spectrum of the dehydrated protein as a function of temperature. If a change in the spectrum occurs upon varying temperature, this suggests that the solvent may not be the primary factor in determining the structure and dynamics of the proteins. With m*AFGP8, a clear difference in the ^{13}C-NMR spectra (MAS and spin-echo) upon freezing is observed. This strongly indicates that the presence of water molecules is critical for this process which, however, is not a surprise, considering their function. At the same time, because there are no chemical shift changes in the freeze-dried m*AFGP in comparison to the hydrated ones (both in D_2O and in H_2O, Table 1), it is unlikely that the conformation of AFGP changes significantly upon hydration. Yet, one cannot rule out any possible changes in the dynamic behavior. The $T_{1\rho}$ and T_{CH} values of both the broad and sharp peaks of freeze-dried m*AFGP8 are the same (3.7 ms and 0.11 ms,

respectively, Table 1), and are distinctly different from those of the hydrated m*AFGP8. At −20°C both the broad and sharp peaks of the dried m*AFGP are the same, while in the hydrated state the dynamics of the two methyl groups are significantly different (Table 1). This suggests that the interactions between AFGP and ice (hydrated state) introduce a differential dynamics associated with the methyl groups. It can be concluded that the local conformational differences of the N-terminal methyl groups are also an outcome of protein-water (ice) interaction. The similarity of the N-methyl chemical shifts in both the freeze-dried and hydrated states permits the conclusion that intermolecular interactions either do not alter the conformation of AFGP or are similar in both samples. The AFGP are dehydrated using conventional lyophilization procedures. This, however, does not remove all the water molecules from the protein, and the "dry" protein contains ~4 wt % water, which may be sufficient for adopting a native conformation.

Dynamics of AFGP in the presence of ice

Protein dynamics can vary over more than several orders of magnitude at room temperature, ranging from below picoseconds to well above seconds. It is reasonably well-accepted that these motions occur in a concerted manner such that, for example, fast motions (picosecond time scale) may act as precursors to other large-amplitude motions (Ansari et al., 1985). The origin of these motions can be broad, especially at low temperatures, such as in this study. Solid-state NMR is especially appropriate for investigating site-specific dynamics of proteins. MAS-NMR experiments average out second rank chemical shift tensors, thus allowing the resonances to be narrow so that different local environments can be easily distinguished. Line shape analysis and measurement of relaxation times in the rotating frame ($T_{1\rho}$) directly correlate with the local dynamics, since an overall rotational diffusion of the proteins in the solid state is not present.

The CP-MAS experiment with varying contact times is a powerful tool to investigate the coherent interaction that is responsible for cross-polarization, as well as the incoherent interaction that allows the spins to relax back to equilibrium. The parameters T_{CH} and $T_{1\rho}$ are representative of the coherent and incoherent processes, respectively, and are based on approximating the cross-polarization dynamics to that of a dipolar coupled heteronuclear spin pair. ^{1}H $T_{1\rho}$ of the broad resonance show notable differences in all three samples and at all temperatures, while the measurements for the sharp peak at −20°C are estimated to be >20 ms. This is an indication that faster time scale motions probably in the microsecond or faster time scale dominate the dynamics of the sharp peak. Lowering the temperature to −80°C results in an increase in the ^{1}H $T_{1\rho}$ of the m*AFGP/D_2O sample (from 2.6 ms to 13.5 ms), with a sharp decrease in the T_{CH} values (from 0.27 ms to 0.15 ms, Table 1). An increase in the $T_{1\rho}$ values suggests a relative increase in the effective size of the AFGP-D_2O system involved in the relaxation process, and the relaxation of the methyl protons will be further aided by the rest of the protons of the protein. Reduction in the T_{CH} could occur for several reasons, including a strengthening of the dipolar coupling due to reduction in the large-scale motions or arising from the presence of multiple conformations (Figs. 2 and 3).

The dynamic parameters of m*AFGP/H_2O appear to be dominated by these of the ice protons when compared with those of m*AFGP/D_2O (Table 1). At −20°C a slight increase in both $T_{1\rho}$ and T_{CH} values of the m*AFGP/H_2O sample is observed. At −80°C, the relaxation of the protons reflects a significant contribution from the H_2O, while the coherent interaction that allows the cross-polarization plays a role similar to that of the m*AFGP/D_2O system. The T_{CH} values show that the rate of transfer of magnetization during the cross-polarization between the ^{1}H and ^{13}C spins in the hydrated states are close to each other. In comparison to freeze-dried m*AFGP at −20°C, the hydrated protein (both in D_2O or H_2O) shows weaker dipolar interaction (larger T_{CH} values) and similar values of $T_{1\rho}$. These results strongly suggest that the interaction between AFGP and ice is not involved in the cross-polarization, but only in the subsequent relaxation process. This further indicates that the AFGP-ice interaction is highly dynamic in nature and occurs in the vicinity of nanoseconds to picosecond time scale, as determined by the spectral density functions of the related $T_{1\rho}$ values. If there are slower time scale motions present (in the picosecond to millisecond time scale), they are not occurring in the N-terminal of AFGP. It is important to note that the dynamic equilibrium between the various conformational states does not interfere with these conclusions as in a spin-locked state, and the system is always in the fast exchange regime ($k_{ex} \ll \Delta\omega_r$, k_{ex} and $\Delta\omega_r$ of the exchange rate and chemical shift difference) (Krishnan and Rance, 1995).

CONCLUSIONS

Although this work does not exactly answer what the mechanism of antifreeze action of these glycoproteins is, it provides valuable information on their dynamics and conformation in the presence of ice. The results are summarized below and are also presented schematically in Fig. 7. 1) The conformation of AFGP in the solution state does not change drastically upon freezing; 2) although the secondary structure in the frozen state is not unique, extended β-conformation and turns appear dominating; 3) the local structure of the freeze-dried protein is similar to that of the fully hydrated protein; 4) the interaction between the AFGP and ice significantly modulates the dynamics of the protein at the chemically modified N-terminus, producing differential effects. Similar kinds of dynamics or additional modulation in the rest of the protein, especially in the side chains, may also

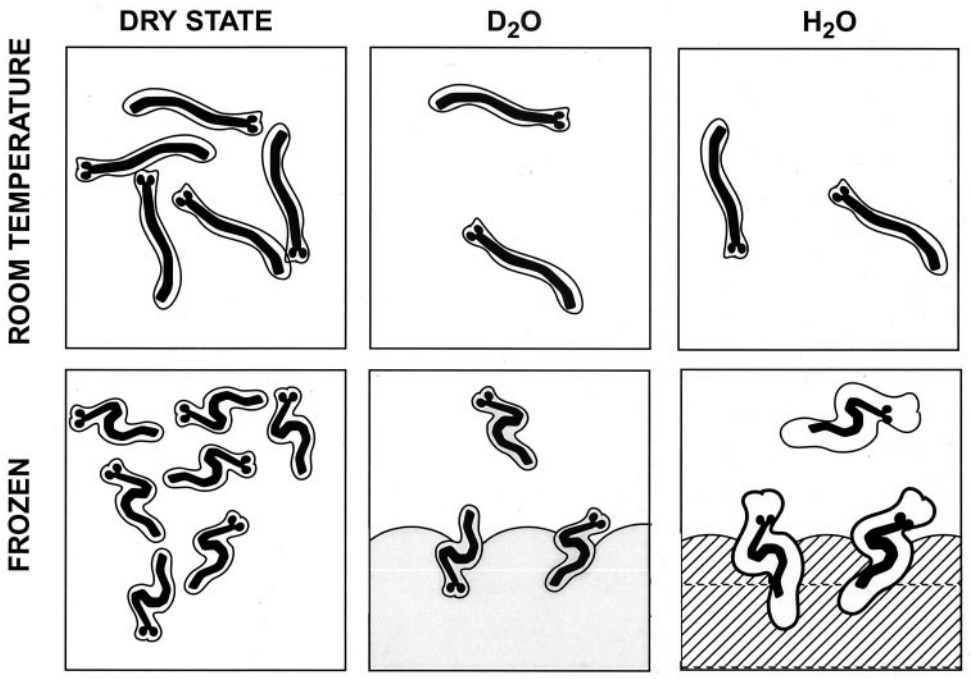

FIGURE 7 Schematic representation of the structure and dynamics of AFGP in the presence of ice as observed by solid-state NMR and FTIR. Chemical modification of the N-terminus by the methyl groups is shown as filled spheres. The size of the envelope covering the AFGP molecule correlates to the relaxation parameters. At room temperature, m*AFGP both in D_2O and H_2O are in the fluid state and the dried protein is in the solid state, whereas all are in the solid state when frozen. The relative orientation of the AFGP molecule on the ice surface is random.

be expected; 5) the time scale of these motions are in the nanosecond to picosecond range; 6) there is a clear distinction between the intramolecular (protein) and intermolecular (protein-water) interaction. Water/ice plays a major role in modulating the motions, and thus in forming a *dynamically constrained* system; 7) within the resolution of these methods, both AFGP8 and AFGP2–5 are dominated by the same kinds of interactions with ice.

The authors are grateful to Drs. Andrew Lane and Willem Wolkers, and to Salvador Zepeda and Dat Nguyen for helpful discussions.

This work was supported by the W. M. Keck Foundation and by Grants R01HL57810-01 and HL61204 from the National Institutes of Health.

REFERENCES

Ansari, A. J., J. Berendzen, S. F. Bowne, H. Frauenfelder, I. E. T. Iben, T. B. Sauke, E. Shyamsunder, and R. D. Young. 1985. Protein states and proteinquakes. *Proc. Natl. Acad. Sci. U.S.A.* 82:5000–5004.

Bandekar, J. 1992. Amide modes and protein conformation. *Biochim. Biophys. Acta.* 1120:123–143.

Berman, E., A. Allerhand, and A. L. DeVries. 1980. Natural abundance carbon 13 nuclear magnetic resonance spectroscopy of antifreeze glycoproteins. *J. Biol. Chem.* 255:4407–4410.

Bush, C. A., and R. E. Feeney. 1986. Conformation of the glycopeptide repeating unit of antifreeze glycoprotein of polar fish as determined from the fully assigned proton n.m.r. spectrum. *Int. J. Peptide Protein Res.* 28:386–397.

Bush, C. A., S. Ralapati, G. M. Matson, R. B. Yamasaki, D. T. Otsuga, Y. Yeh, and R. E. Feeney. 1984. Conformation of antifreeze glycoprotein of polar fish. *Arch. Biochem. Biophys.* 232:624–631.

Byler, D. M., and H. Susi. 1986. Examination of the secondary structure of proteins by deconvolved FTIR spectra. *Biopolymers.* 25:469–487.

Chirgadze, Y. N., O. V. Fedorov, and N. P. Trushina. 1975. Estimation of amino acid residue side-chain absorption in the infrared spectra of protein solutions in heavy water. *Biopolymers.* 14:679–694.

Davies, P. L., and C. L. Hew. 1990. Biochemistry of antifreeze proteins. *FASEB J.* 4:2460–2468.

DeVries. A. L. 1986. Antifreeze glycoproteins and peptides: interactions with ice and water. *Methods Enzymol.* 127:293–303.

DeVries, A. L., S. K. Komatsu, and R. E. Feeney. 1970. Chemical and physical properties of freezing point-depressing glycoproteins from Antarctic fishes. *J. Biol. Chem.* 245:2901–2908.

Dong, A., P. Huang, and W. S. Caughey. 1990. Protein secondary structures in water from second-derivative amide I infrared spectra. *Biochemistry.* 29:3303–3308.

Doucet, C. J., L. Byass, L. Elias, D. Worrall, M. Smallwood, and D. J. Bowles. 2000. Distribution and characterization of recrystallization inhibitor activity in plant and lichen species from the UK and maritime Antarctic. *Cryobiology.* 40:218–227.

Drewes, J. A., and K. L. Rowlen. 1993. Evidence for a γ-turn motif in antifreeze glycopeptides. *Biophys. J.* 65:985–991.

Duman, J. G. 2001. Antifreeze and ice nucleator proteins in terrestrial arthropods. *Annu. Rev. Physiol.* 63:327–357.

Duman, J. G., N. Li, D. Verleye, F. W. Goetz, D. W. Wu, C. A. Andorfer, T. Benjamin, and D. C. Parmelee. 1998. Molecular characterization and sequencing of antifreeze proteins from larvae of the beetle *Dendroides canadensis. J. Comp. Physiol. B.* 168:225–232.

Ewart, K. V., Q. Lin, and C. L. Hew. 1999. Structure, function and evolution of antifreeze proteins. *Cell. Mol. Life Sci.* 55:271–283.

Feeney, R. E. 1988. Inhibition and promotion of freezing: fish antifreeze proteins and ice-nucleating proteins. *Comm. Agric. Food Chem.* 1:147–181.

Feeney, R. E., T. S. Burcham, and Y. Yeh. 1986. Antifreeze glycoproteins from polar fish blood. *Annu. Rev. Biophys. Biophys. Chem.* 15:59–78.

Feeney, R. E., and Y. Yeh. 1978. Antifreeze proteins from fish blood. *Adv. Protein Chem.* 32:191–281.

Filira, R., L. Biondi, B. Scolaro, M. T. Foffani, S. Mammi, E. Peggion, and R. Rocchi. 1990. Solid phase synthesis and conformation of sequential glycosylated polytripeptide sequences related to antifreeze glycoproteins. *Int. J. Biol. Macromol.* 12:41–49.

Geoghegan, K. F., D. T. Osuga, A. I. Ahmed, Y. Yeh, and R. E. Feeney. 1980. Antifreeze glycoproteins from polar fish. Structural requirements for function of glycoprotein 8. *J. Biol. Chem.* 255:663–667.

Graether, S. P., M. Kuiper, S. M. Gagne, V. K. Walker, Z. Jia, B. D. Skyes, and P. L. Davis. 2000. β-Helix structure and ice-binding properties of a hyperactive antifreeze protein from an insect. *Nature.* 406:325–328.

Harding, M. M., L. G. Ward, and A. D. J. Haymet. 1999. Type I "antifreeze" proteins. *Eur. J. Biochem.* 264:653–665.

Haymet, A. D. J., L. G. Ward, and M. M. Harding. 1999. Winter flounder "antifreeze" proteins: synthesis and ice growth inhibition of analogs that probe the relative importance of hydrophobic and hydrogen-bonding interactions. *J. Am. Chem. Soc.* 121:941–948.

Homans, S. W., A. L. DeVries, and S. B. Parker. 1985. Solution structure of antifreeze glycopeptides. Determination of the major conformers of the glycosidic linkages. *FEBS Lett.* 183:133–137.

Knight, C. A., C. C. Cheng, and A. L. DeVries. 1991. Adsorption of α-helical antifreeze peptide on specific ice crystal surface planes. *Biophys. J.* 59:409–418.

Knight, C. A., E. Driggers, and A. L. DeVries. 1993. Adsorption to ice of fish antifreeze glycopeptides 7 and 8. *Biophys. J.* 64:252–259.

Komatsu, S. K., A. L. DeVries, and R. E. Feeney. 1970. Studies of the structure of freezing point-depressing glycoproteins from Antarctic fish. *J. Biol. Chem.* 245:2909–2913.

Krishnan, V. V., and M. Rance. 1995. Influence of chemical exchange among homonuclear spins in heteronuclear coherence-transfer experiments in liquids. *J. Magn. Reson. S.A.* 116:97–106.

Lane, A. N., L. M. Hays, R. E. Feeney, L. M. Crowe, and J. H. Crowe. 1998. Conformational and dynamic properties of a 14 residue antifreeze glycopeptide from Antarctic cod. *Protein Sci.* 7:1555–1563.

Lane, A. N., L. M. Hays, N. M. Tsvetkova, R. E. Feeney, L. M. Crowe, and J. H. Crowe. 2000. Comparison of the solution conformation and dynamics of antifreeze glycoproteins from Antarctic fish. *Biophys. J.* 78:3195–3207.

Liou, Y-C., A. Tocilj, P. Davies, and Z. Jia. 2000. Mimicry of ice structure by surface hydroxyls and water of a β-helix antifreeze protein. *Nature.* 406:322–325.

Means, G. E., and R. E. Feeney. 1995. Reductive alkylation of proteins. *Anal. Biochem.* 224:1–16.

Osuga, D. T., and R. E. Feeney. 1978. Antifreeze glycoproteins from arctic fish. *J. Biol. Chem.* 253:5338–5343.

Prestrelski, S. J., D. M. Byler, and M. N. Liebman. 1991. Comparison of various molecular forms of bovine trypsin: correlation of infrared spectra with x-ray crystal structures. *Biochemistry.* 30:133–143.

Rao, B. N. N., and C. A. Bush. 1987. Comparison by ^{1}H-NMR spectroscopy of the conformation of the 2600 Dalton antifreeze glycopeptide of polar cod with that of the high molecular weight antifreeze glycoprotein. *Biopolymers.* 26:1227–1244.

Raymond, J. A., and A. L. DeVries. 1977. Adsorption inhibition as a mechanism of freezing resistance in polar fishes. *Proc. Natl. Acad. Sci. U.S.A.* 74:2589–2593.

Raymond, J. A., P. Wilson, and A. L. DeVries. 1989. Inhibition of growth of nonbasal planes in ice by fish antifreezes. *Proc. Natl. Acad. Sci. U.S.A.* 86:881–885.

Sidebottom, C., S. Buckley, S. P. Pudney, S. Twigg, C. Jarman, C. Holt, J. Telford, A. McArthur, D. Warrall, R. Hubbard, and P. Lillford. 2000. Heat-stable antifreeze protein from grass. *Nature.* 406:256.

Sönnichsen, F. D., P. L. Davies, and B. D. Sykes. 1998. NMR structural studies on antifreeze proteins. *Biochem. Cell Biol.* 76:284–293.

Surewicz, W. K., and H. H. Mantsch. 1988. New insight into protein secondary structure from resolution-enhanced infrared spectra. *Biochim. Biophys. Acta.* 952:115–130.

Surewicz, W. K., H. H. Mantsch, and D. Chapman. 1993. Determination of protein secondary structure by Fourier transform infrared spectroscopy: a critical assessment. *Biochemistry.* 32:389–394.

Tomimatsu, Y., J. R. Scherer, Y. Yeh, and R. E. Feeney. 1976. Raman spectra of a solid antifreeze glycoprotein and its liquid and frozen aqueous solutions. *J. Biol. Chem.* 251:2290–2298.

Udenfriend, S., S. Stein, P. Bohlen, and W. Dairman. 1972. Fluorescamine: a reagent for assay of amino acids, peptides, proteins, and primary amines in the picomole range. *Science.* 178:871–872.

van Gorkom, L. C. M., J. M. Hook, M. B. Logan, J. U. Hanna, and R. E. Wasylishen. 1995. Solid-state lead-207 NMR of lead (II) nitrate: localized heating effects at high magic angle spinning speeds. *Magn. Res. Chem.* 33:791–795.

Wen, D., and R. A. Laursen. 1992. A model for binding of an antifreeze polypeptide to ice. *Biophys. J.* 63:1659–1662.

Wilson, P. W., D. Beaglehole, and A. L. DeVries. 1993. Antifreeze glycopeptide adsorption on single crystal ice surface using ellipsometry. *Biophys. J.* 64:1878–1884.

Yeh, Y., and R. E. Feeney. 1996. Antifreeze proteins: structures and mechanisms of function. *Chem. Rev.* 96:601–617.